Powder Technology 192 (2009) 375–383

Contents lists available at ScienceDirect

Powder Technology

journal homepage: www.elsevier.com/locate/powtec

Preparation of double layered shell microparticles containing an acid dye by a melt dispersion–coacervation technique

Fabien Salaün *, Isabelle Vroman, Carole Aubry

Laboratoire de Génie et Matériaux Textiles (GEMTEX), UPRES EA2461, École Nationale Supérieure des Arts et Industries Textiles (ENSAIT), BP 30329, 59056 Roubaix Cedex 01, France

ARTICLE INFO

Article history:
Received 9 May 2008
Received in revised form 6 December 2008
Accepted 26 January 2009
Available online 3 February 2009

Keywords:
Microencapsulation
Melt dispersion–coacervation
Acid dye
Carnauba wax

ABSTRACT

Two types of microparticles with a double layered shell containing an acid dye were prepared by using a melt dispersion–coacervation process. The surface morphology and the composition of the microcapsules were investigated using scanning electron microscope (SEM), and Fourier-transform infrared spectroscope (FTIR) respectively. The results showed that the loading content and morphologies strongly depend on the composition, the protective colloid, as well as on the outer polymeric shell and the way the solvent solubilizes it. The thermo-physical properties strongly depend on the nature of the core content and the synthesis conditions. Factors affecting the release performance of the microcapsules were investigated and the results are presented in this paper.

1. Introduction

The application of microencapsulated dye technology in textile dyeing and printing has been investigated since early 90s [1]. Microcapsules are tiny particles in the size range of 1 μm to 2 mm surrounding functional materials with a polymer shell. The release properties of the polymer that forms the shell depends on the class of the wall materials, but also on the microencapsulation methods, on the physico-chemical parameters of the process, on the mean particle size and on the membrane thickness [2,3]. In recent years, composite microparticles comprising of polymeric matrixes embedded with dye have attracted much interest in the field of dyeing textiles [4].

The water-soluble anionic dyes, which are one of the most important groups of dyes used in the textile dyeing industries, are used to dye fabrics like wool, nylon and silk. Microencapsulation of dyes allows them to be protected from the outside environment. It also allows them to have a reduced reactivity and so ensures good dyeing characteristics [4]. Up to now, reactive and dispersed dye were essentially encapsulated by interfacial polymerization in polyurea and polyurethane shell [5–10] or in a liposomic structures [11] whereas acid dyes were only entrapped in a liposomic structure [12,13].

Core-shell microcapsules have been investigated widely and significant promise for providing new functionalities was shown. Thus, many "smart" microparticles have been synthesized to act in response to the change in environmental stimuli, e.g. temperature [14–17], pH[18], light [19,20], electric [21] or magnetic field [22], and other stimuli. The microparticles using a single polymer shell present certain numbers of disadvantages including an initial burst, caused by the release of the active substance trapped on the surface during the encapsulation process and a low encapsulation efficiently for highly water soluble compound. The addition of a second polymer layer to a polymeric microparticle to form a two-layered structure may overcome these limitations. Thus these structures may provide the opportunity to improve the thermal conductivity and stability of the particles [23,24]. Furthermore, the selection of the appropriate core and the appropriate shell polymer chemistries plays an important role to control the release of the active substance [25] and to incorporate the particles on a substrate [26]. One of the possible ways to achieve the linkage on a textile substrate is to fuse the outer thermoplastic wall by a "hot-melt" process.

Various approaches have been designed to prepare this two-layered polymer blend structure to obtain required properties. One method entails a polymer–polymer phase separation of a binary blend of polymer solutions, which results in the formation of double walled microparticles [27]. Another method is to encapsulate active substance in microparticles using conventional microencapsulation technique and then coat these particles with a second polymer. With the formation of the outer coating, the active substance diffusion and the burst effect during the process are reduced since no active substance is entrapped on the surface of the particles [28].

Gander et al. [29] have shown that the morphology of the microparticles depended on the polymer solvent system. One method predicting the solubility of a solute in a solvent is to compare their solubility parameters. Thus, a good solvent for a solute such as a polymer has a solubility parameter close to that of the solute's one.

* Corresponding author. ENSAIT-GEMTEX, 9 rue de l'ermitage, BP 30329, 59100 Roubaix, France. Tel.: +33 3 20 25 64 59; fax: +33 3 20 27 25 97.
E-mail address: fabien.salaun@ensait.fr (F. Salaün).

0032-5910/$ – see front matter © 2009 Elsevier B.V. All rights reserved.
doi:10.1016/j.powtec.2009.01.018

Hildebrand or partial Hansen solubility parameters (δ_t, δ_d, δ_p, δ_h) can be used for predicting polymer/solvent properties.

In this work, we have checked the ability to synthesize microcapsules containing acid dye with an uncoloured shell: once the microcapsules are applied on the textile support, the colorant is released by melting the microcapsule shells forming specks which can penetrate the textile. The microparticles were prepared using a melt dispersion-coating method. Gelatin, a natural macromolecule, is widely used in biomedical and biotechnological applications and is a good candidate for preparation of microspheres and microcapsules for the purpose of controlled release applications of drugs. The aim of this study was to prepare microcapsules containing a water-soluble dye used in the textile industry which changes colour irreversibly according to the external environmental conditions. Microencapsulated acid dyes have been characterised in terms of thermal properties measured by Differential Scanning Calorimeter (*DSC*), morphological structure (SEM), chemical composition (FTIR) and colour differences (E^*) using spectrophotometer.

2. Experimental

2.1. Materials

Commercial grade dye AR57 (Nylosan Red EBL) was supplied by Clariant-Switzerland and used without further purification. Carnauba wax, poly(vinyl alcohol) (M.W. 95000, 95% hydrolysed), gelatine used as emulsifiers and span 85, employed as surfactant, were purchased from Acros Organics and Aldrich, respectively. Carnauba wax belongs to the naturally occurring waxes of vegetable origin, which constitutes mainly high molecular weight esters [30,31]. Low density polyethylene (PE) and polystyrene (PS) were obtained from Elf Atochem and BP chemicals respectively. Toluene, Chloroform and Petroleum ether from Aldrich are used as received.

2.2. Methods

2.2.1. Solvent selection

Carnauba wax was used as the encapsulating material. Ten organic solvents having a Hansen solubility parameter of 14–27 $MPa^{1/2}$ were screened for polymer solvency (Table 1). 1 g of carnauba wax was added to test tubes containing 10 ml of the test organic solvent. The test tubes were agitated during 2 h at 50 °C. Solubility of carnauba was judged by visual examination. Solvents were classified into four groups: good solvents that formed clear wax solutions; intermediately good solvents that formed turbid wax solutions; intermediately poor solvents that were marginally able to swell the wax; and poor solvents in which the carnauba wax remained intact.

The Hansen solubility parameters consist of three components, with a dispersion term δ_D, a polar term δ_P, and a hydrogen-bonding term δ_H, which together make up the total solubility parameter δ_t, and their relationship can be expressed as in Eqs. (1) and (2):

$$\delta_t^2 = \delta_d^2 + \delta_p^2 + \delta_h^2 \tag{1}$$

$$\delta_t = \sqrt{\frac{E}{V}} \tag{2}$$

Where, E is the vaporization energy of the solvent, and V is the molar volume of a solvent. Solubility parameters are not available for carnauba wax. In this case, the calculation of Hansen solubility parameters can be estimated by incremental methods. There are based on group attraction constants F_{Di} and F_{Pi}, for dispersion and polar components, and group cohesion energies E_{Hi}. The contributions of the different groups to the cohesion energy and the molar volume have been published by Fedors [32] and corresponding solubility parameters can be calculated by means of Eqs. (3), (4) and (5).

Table 1
Solubility parameter components of various solvents and interaction radius.

Solvent	δ_d ($MPa^{1/2}$)	δ_p ($MPa^{1/2}$)	δ_h ($MPa^{1/2}$)	δ_h ($MPa^{1/2}$)	R_{ij}
Acetone	15.5	10.4	7.0	19.9	11.2
Chloroform	17.8	3.1	5.7	18.9	4.9
Cyclohexane	16.8	0	0.2	16.8	2.2
Dichloromethane	18.2	6.3	6.1	20.2	7.6
Ethanol	15.8	8.8	19.4	26.5	19.1
Ethyl acetate	15.8	5.3	7.2	18.2	7.0
Hexane	14.9	0.0	0.0	14.9	4.1
Petroleum ether	15.2	0.0	0.0	15.2	3.7
Toluene	18.0	1.4	2.0	18.2	3.0
Xylene	17.8	1	3.1	18.1	2.6

$$\delta_d = \frac{\Sigma_i F_{Di}}{\Sigma_i V_i} \tag{3}$$

$$\delta_p = \frac{\sqrt{\Sigma_i {F_{Pi}}^2}}{\Sigma_i V_i} \tag{4}$$

$$\delta_H = \sqrt{\frac{\Sigma_i E_{Hi}}{\Sigma_i V_i}} \tag{5}$$

The chemical composition of carnauba is complex, and the different components can be fallen into five classes such as fatty acids, ω-hydroxy fatty acids, alcohols, α,ω-diols and cinammic acids [33]. Thus, in this study, to calculate the solubility parameters from Hansen theory, we consider that carnauba wax is composed almost entirely of esters of C_{24}, C_{26} and C_{28} carboxylic acids and C_{30}, C_{32} and C_{34} straight-chained primary alcohols and contains more essentially myricyl cerotate ($C_{25}H_{51}COOC_{30}H_{61}$) and small quantities of free cerotic acid ($CH_3(CH_2)_{24}COOH$) and myricyl alcohol ($C_{30}H_{61}OH$) [33].

Furthermore, according to Hansen, the region of good solubility can be characterized by the distance between solvent and polymer and defined as a sphere in the three-dimensional space of the solubility parameters. The corresponding interaction radius for solvent i and polymer j is therefore given by Eq. (6):

$$R_{ij} = \left[4\left(\delta_{d,i} - \delta_{d,j}\right)^2 + \left(\delta_{p,i} - \delta_{p,j}\right)^2 + \left(\delta_{h,i} - \delta_{h,j}\right)^2\right]^{\frac{1}{2}} \tag{6}$$

This means that a polymer is probably soluble in a solvent if the Hansen parameters for the solvent lie within the solubility sphere for the polymer. In order to predict the solubility, the distance R_{ij} must be less than the interaction radius of the polymer, R_j. Here, we replaced the polymer by carnauba wax. Thus, the calculated Hansen solubility parameters of carnauba wax are $\delta_d = 16.6$ $MPa^{1/2}$, $\delta_p = 0.5$ $MPa^{1/2}$, $\delta_h = 2.3$ $MPa^{1/2}$ and $\delta_t = 16.8$ $MPa^{1/2}$.

2.2.2. Preparation of double-walled microparticles

The microencapsulation of an acid dye was carried out in a 500 ml three neck round-bottomed flask equipped with a mechanical stirrer by a melt dispersion–coacervation technique. Typical procedure for the preparation of double layered shell microcapsules was divided in two steps in which firstly, spherical particles were prepared by using carnauba according to the w/o melt dispersion method, and secondly these later were entrapped with a surrounding polymer either PS or PE by a coacervation-phase separation technique induced by the addition of a non-solvent either ethanol or water (Fig. 1).

2.2.2.1. Preparation of microparticles. 40 ml of an aqueous phase containing an acid dye solution (1%-wt) and 0, 0.33, 0.66, 1.33 or 3.33%-wt of gelatin were emulsified at 900 rpm with a mechanical

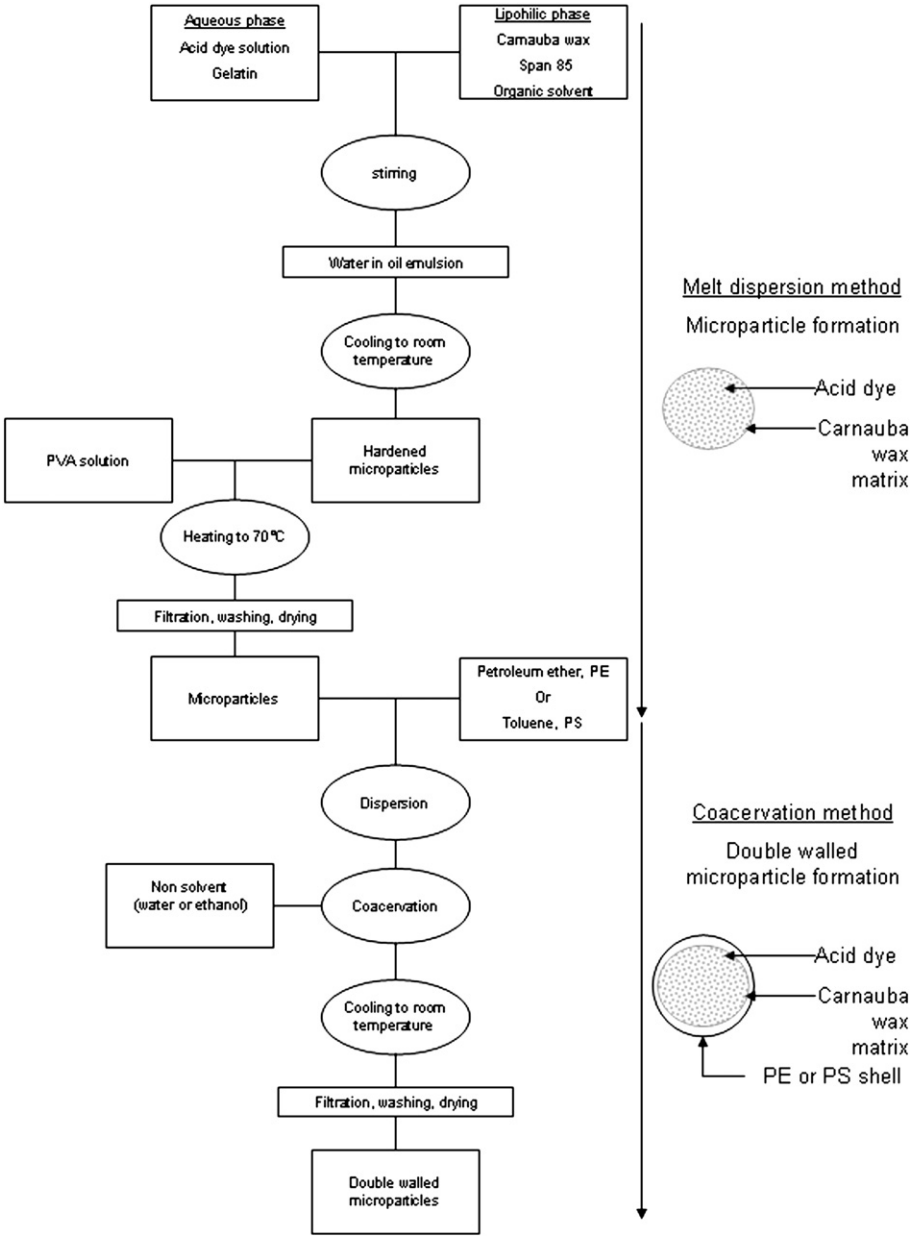

Fig. 1. Schematic representation of the microencapsulation process.

stirrer in a lipophilic phase for 2 min at 75 °C. The lipophilic phase consisted of 50 g of carnauba wax and 3 g of Span 85 were dissolved in 50 ml of organic solvent either cyclohexane or toluene. The hardening of the droplets was performed by decreasing the temperature at a cooling rate of 5 °C/min until room temperature under a constant stirring at 300 rpm. The resulting dispersion was added dropwise to 200 ml of PVA solution containing 1% (w/v) of PVA. Then the temperature was gradually raised up to 70 °C during 1 h. Finally, the microparticles were washed with water, filtered and dried at 35 °C overnight.

2.2.2.2. Formation of outer wall. 40 g of the resultant microparticles were dispersed either in 50 ml of petroleum ether or in 50 ml of toluene with 6 g of PE or PS respectively under 900 rpm at 80 °C or 60 °C according to the polymer choice. Coacervation was induced by introducing dropwise a predetermined amount of a non solvent, water for PE and ethanol for PS. The hardening of the coacervated microparticles was performed by decreasing temperature to room temperature until the microparticles were sufficiently hardened to be filtered, washed and dried for storage.

2.2.3. Microparticles characterizations

2.2.3.1. Dye diffusion. The dye concentration was determined by spectrophotometric assessment conducted on a JASCO V530 spectrophotometer at the wavelength of maximum absorption of the dye (λ_{max}) in water (513 nm), cyclohexane and toluene (550 nm) using a calibration curve of absorption.

Dye diffusion in toluene-carnauba wax medium was determined from the absorbances of a series of solutions containing a fixed concentration of dye ($C_{dye} = 2 \times 10^{-4}$ mol dm^{-3}) and increasing concentration of gelatin from 0 to 3.33%-wt. The amount of non-entrapped dye was determined by spectrophotometry. Absorbance values obtained at λ_{max}, can be also used for the estimation of dye

diffusion in solvent. We used this method to determine the dye diffusion in the continuous phase during the microencapsulation process after the microparticle formation. Continuous phase (toluene or cyclohexane) containing free dye was separated from solid microparticles by centrifugation. In order to remove the possible residual small particles which do not settle down during centrifugation, a second filtration of the supernatant was done using a Büchner system.

2.2.3.2. Chemical characterization. The composition of the shell polymer was analyzed by FT-IR spectra. Samples were ground and mixed with KBr to make pellets. FTIR spectra in the transmission mode were recorded using a Nicolet Nexus, connected to a PC, in which the number of scan was 32 and the resolution was 4 cm^{-1}.

2.2.3.3. Scanning electron microscopy. The surface morphology of the microcapsules was observed with the help of a scanning electron microscopy (Philips XL30 ESEM / EDAX- SAPPHIRE) at an accelerated voltage of 15 kV.

2.2.3.4. Thermal characterization. The thermal behavior of the particles was recorded using a TA instrument type DSC 2920 piloted on PC with TA Advantage control software. Indium was used as standard for temperature calibration and the analysis was made under a constant stream of nitrogen (50 ml/min). Samples were placed in aluminum pans which were hermetically sealed before being placed on the calorimeter thermocouples. The sample space was purged with nitrogen at a constant flow (50 ml/min) during the experiments. The temperature range was from −30 to 100 °C at a rate of 1°/min with 5 mg. Reproducibility was tested by three measurements. The mean deviation was ±0.1 °C in melting and crystallization temperatures, and ±0.3, ±0.4 and ±0.3 J/g in latent heat of carnauba wax, microparticles and double walled microspheres, respectively.

2.2.3.5. Loading content and encapsulation efficiency. The amounts of AR57 encapsulated into carnauba microspheres (first stage of the preparation) and carnauba/PE (or carnauba/PS) microspheres (second stage of the preparation) were determined by thermal analysis. All experiments were performed in triplicate. The specific heat of carnauba wax was a constant in the measured temperature range. The content of dye in the carnauba microspheres can be estimated according to the measured enthalpy:

$$\text{dye content}(\%) = 100 - \frac{\Delta H_{\text{acid dye / carnauba wax microsphere}}}{\Delta H_{\text{carnauba wax}}} \times 100\% \quad (7)$$

Where $\Delta H_{\text{acid dye / carnauba wax microsphere}}$ is the enthalpy (crystallization enthalpy) of microspheres (J g^{-1}), $\Delta H_{\text{carnauba wax}}$ the enthalpy (melting or crystallization) of carnauba wax. In this study, the enthalpies of melting and crystallization are 204.2 J g^{-1} and 199.2 J g^{-1}, respectively.

The content of dye in the carnauba/PE and carnauba/PS microspheres was calculated as follows:

$$\text{dye content}(\%) = 100 - \frac{\Delta H_{\text{acid dye/ carnauba wax / PE or PS microspheres}}}{\Delta H_{\text{carnauba wax / PE or PS microspheres}}} \times 100\% \quad (8)$$

Where $\Delta H_{\text{acid dye / carnauba wax / PE or PS microspheres}}$ and $\Delta H_{\text{carnauba wax / PE or PS microspheres}}$ are the enthalpy (crystallization enthalpy) of microspheres with and without acid dye, respectively.

The PE and PS content in the carnauba microspheres were calculated from the ratio of the measured values of carnauba/PE (or PS) microspheres to carnauba wax enthalpy. From the amounts introduced, the theoretical content was found to be about 10.7%-wt.

2.2.3.6. Colour measurement. The reflectance and CIELAB values of the dried samples were measured on a Datacolor International SF 600 plus interfaced with a personal computer. The colour difference (ΔE) between the acid dye and the various microparticles was obtained from the distance between their coordinates in CIELAB colour space using the following equation:

$$\Delta E = \sqrt{\Delta L^{*2} + \Delta a^{*2} + \Delta b^{*2}} \quad (9)$$

where L^*, a^* and b^* are colour coordinates of the samples, ΔL^*, Δa^* and Δb^* are the differences between the corresponding parameters of

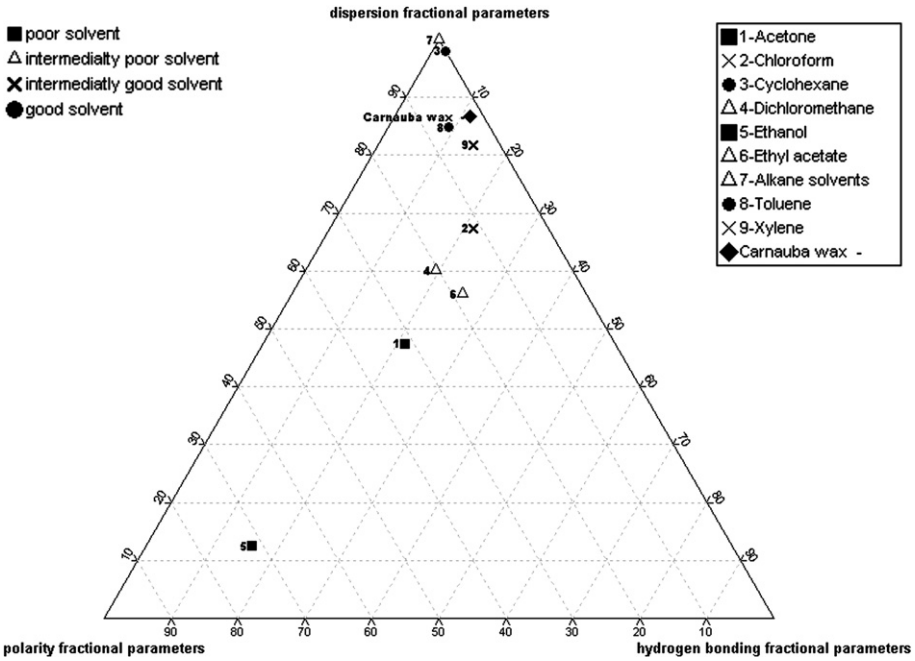

Fig. 2. Comparison of Hansen's solubility parameters for various solvents: contributions of dispersion forces (f_d), polar interactions (f_p), and hydrogen bonding (f_h).

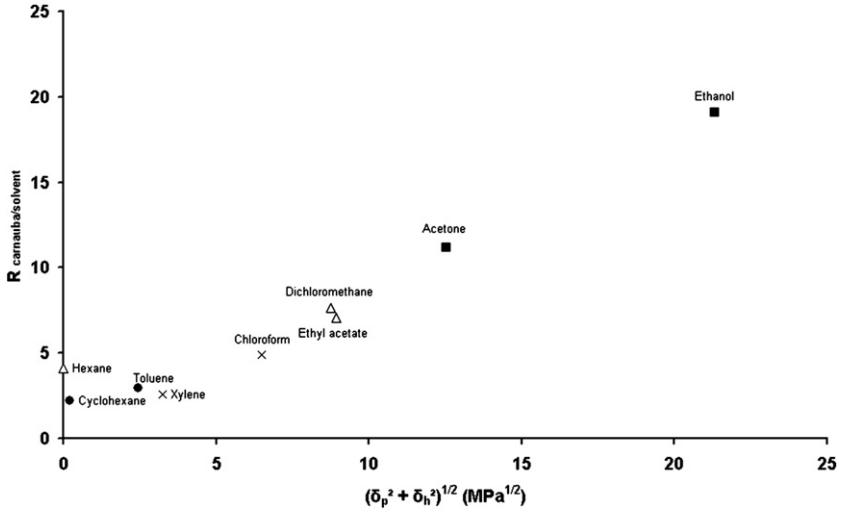

Fig. 3. Effect of the hydrogen bonding force and polar components on interaction radius.

samples and standard. Readings were taken at three different locations. Average values and standard deviations were taken.

3. Results and discussion

3.1. Solvent selection

Ten organic solvents with solubility parameters of 14–27 MPa$^{1/2}$ were tested to evaluate solubilization of carnauba wax. The results were summarized on a triangular graph using the method of Teas [34], as shown in Fig. 2. As described by Teas, the fractional parameters of each solvent were calculated from Eq. (10) and were displayed on a triangular plot.

$$f_i = \frac{\delta_i}{\delta_d + \delta_p + \delta_h} \tag{10}$$

Where, $i = d$, p, h, and δ_d, δ_p, and δ_h are Hansen's multicomponent solubility parameters and represent the contributions from dispersion forces, polar interactions, and hydrogen bonding, respectively.

In the triangular graph shown in Fig. 2, solvents which produced clear solutions of carnauba wax are also localized in a region of relatively low f_p and f_h but of high f_d of the plot. Solvents lying outside of this area of solubility were found to be mostly poor or nonsolvents for carnauba wax. The position of toluene, cyclohexane, chloroform, xylene and hexane (or petroleum ether) is near to the position of carnauba wax. Furthermore, the best results obtained from the solubility test correspond to toluene and cyclohexane, whereas carnauba wax is only swelled in xylene and chloroform. Solvents such as hexane that have no f_p and f_h values are intermediately poor solvents for carnauba wax even though their solubility parameters are fairly close to the wax's ones. These results show that the solubility of carnauba wax in a given solvent is not only linked to the closeness of the values of their solubility parameters but also to the nature of the internal cohesive forces existing in the material. Thus, the presence of saturated fatty acids and saturated primary alcohols in carnauba wax contribute to hydrogen bonding interactions and solvents without δ_h component (hexane or petroleum ether) are unable to dissolve the wax easily.

The sphere radii of the carnauba wax observed for the carnauba-solvent couple using Hansen solubility parameters of the solvent (Table 1) have been calculated from Eq. (6). As a result, most of solvents dissolving carnauba wax are included in the spherical region with R_{ij} about 5. Since the dispersive component parameters of both solvent and carnauba wax are quite similar, the graphical representation of the corresponding interaction radius can be reduced to a 2-D plot of R_{ij} versus δ_h and δ_p (Fig. 3). The values of interaction radius

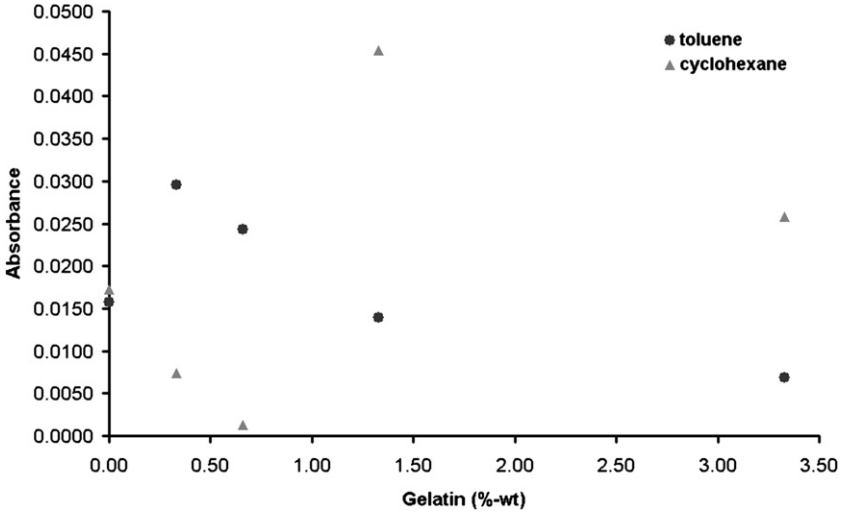

Fig. 4. Effect of the gelatin concentration on released dye amount.

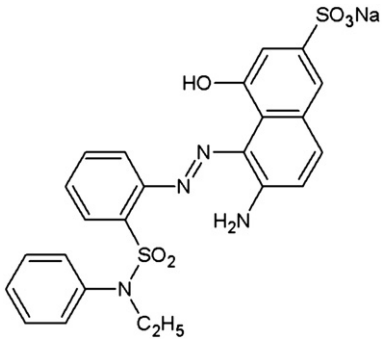

Fig. 5. The structure of AR57.

increase with hydrogen bonding and polar interactions (δ_h and δ_p) values of various solvents. These results suggested that the corresponding interaction radius become higher with an increase in the polar and hydrogen bonding components of the solvent. The observed apparent solubility actually corresponded to the prediction by the interaction radius. Thus, it was also confirmed that the interaction radius could be also applied to predict the apparent solubility of carnauba wax in various organic solvents. From the above study, carnauba wax was found to maximum solubility in cyclohexane followed by toluene, xylene and chloroform.

3.2. Influence of gelatin on dye diffusion during the preparation of microparticles

The formation of microparticles is greatly affected by the emulsifier, which influences the emulsion stability. The emulsifiers used in this process have two main functions: first, to reduce interfacial tension between aqueous and lipophilic phases; second to absorb on the aqueous/organic interface in order to form a layer around the dispersed droplets to prevent the droplets from coalescing and dye diffusion. In this work, gelatin was used as a protein emulsifier. Chemical reactivity of proteins depends on the side chain, the amino acid composition and the free amino and carboxyl groups [35]. The most reactive protein groups are serine (primary –OH), hydroxyproline (secondary –OH), threonine (secondary –OH), tyrosine (phenolic –OH), aspartic acid (–COOH), glutamic acid (–COOH), lysine ($-NH_2$) and arginine ($-C(NH)NH_2$) [36–38].

The Fig. 4 shows the absorbance of cyclohexane and toluene after formation of acid dye / carnauba wax microparticles, e.g. the dye diffusion in the continuous phase before the addition of PVA solution in the first step of the microencapsulation process. The difference between these absorbances can be attributed to the difference of the initial condition especially to the gelatine concentration at the initial state; dye droplets are assumed to be homogeneously distributed in the carnauba microparticle. These results show that the dye release property of carnauba microparticles varies depending on the concentration of gelatin and the choice of the lipophilic phase solvent. Thus, for low concentration of gelatin (<1%-wt), the absorbance of toluene phase is higher than without gelatin. This phenomenon can be related to a destabilization of the system during the process promoting the dye diffusion. The increase of gelatine concentration allows to reduce the absorbance of toluene phase and therefore the dye diffusion. The results obtained with cyclohexane are quite different. Thus, a decrease of absorbance is observed for low concentrations of gelatin, while from 1.33 to 3.33%-wt measured values increase. Therefore, the solubilization of carnauba wax affects the dye diffusion and low amounts of gelatin are required with the best solvent (cyclohexane) than with toluene. Gelatin acts as a protective colloid during the process and stabilizes the dye droplets or particles in the carnauba wax matrix.

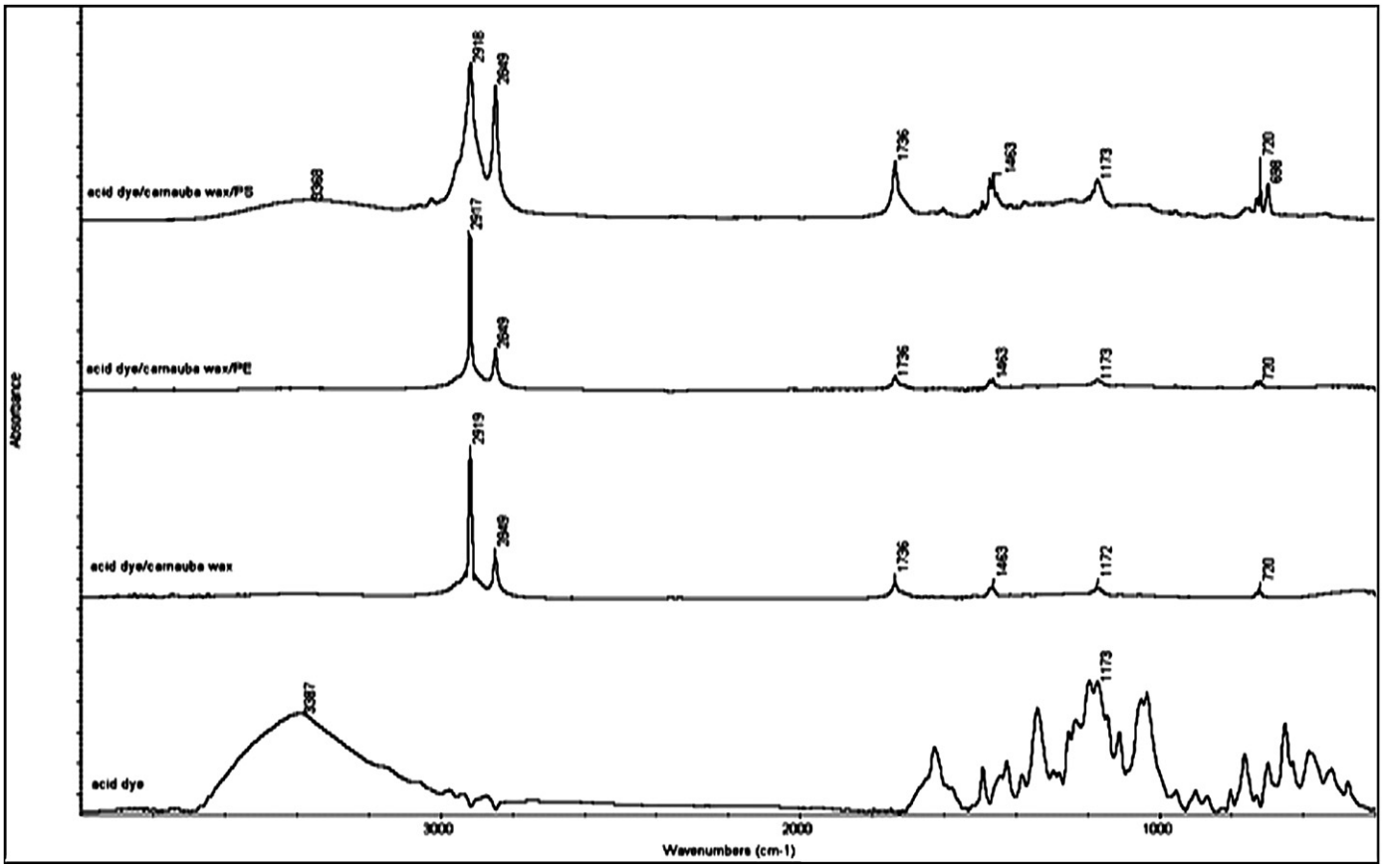

Fig. 6. FTIR spectra of acid dye, acid dye/carnauba wax, acid dye/carnauba wax/PE, acid dye carnauba wax/PS microspheres.

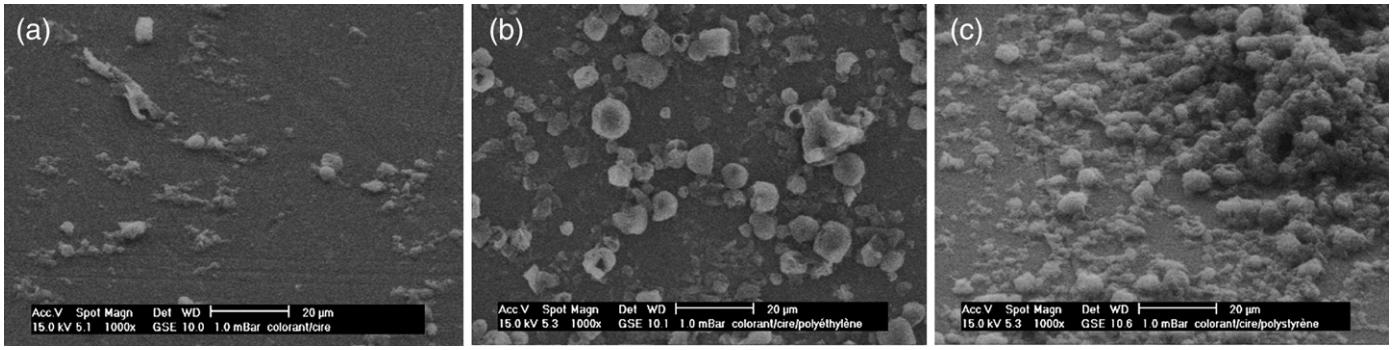

Fig. 7. SEM micrograph of acid dye/wax (a), acid dye/wax/polyethylene (b), acid dye/wax/polystyrene (c) microspheres at a magnification of 1000.

This effect is strongly dependent on the interactions between the amino content of the gelatine and the anionic sites of the dye at pH 5.

The chemical structure of the AR 57 (Fig. 5) shows that this dye should produce a strongly ionizable sulfonate group at low pH. Acid dye can be expected to interact with groups, such as amino, hydroxy, carbonyl and amino, present in the gelatin, by virtue of various ionic and non-ionic forces of interaction (e.g. hydrogen bonding, dispersion forces, dipole–dipole and electrostatic forces). At pH 5, the sulfonate groups of the dye dissociate and are converted to dye anions. At the pH of the emulsion, which was 3 units below the isoelectric point of the gelatin, the gelatin was a cationic polyelectrolyte. Therefore, protonated amino groups along the gelatin chain can act as dye sites for anionic dyes. Indeed, more protons will be available, thereby increasing electrostatic attractions between negatively charged dye anions and positively charged adsorption sites and causing an increase in dye adsorption. Therefore, gelatine adsorbs dye anion strongly by ionic interaction between $-NH_3^+$ and $-SO_3^-$. Thus, the most probable mechanism of the interaction between gelatin and dye is likely to be ionic interaction of the dye ions with the amino groups of gelatine.

3.3. Structure of microparticles

Spectra of carnauba wax, AR57 and the microparticles are presented in Fig. 6 to identify various core and shell microcapsules via known characteristic wavenumbers. The infrared spectrum of carnauba wax exhibited the strong symmetric and asymmetric CH_2 stretch vibrations at 2848 cm^{-1} and 2920 cm^{-1} respectively. The strong band in the infrared spectrum at 1734 cm^{-1}, is assigned to a C=O vibration, which could be an indication of the presence of esters in this wax and confirms the presence of long-chain aliphatic ketone or fatty acid [39]. It is seen that the $-(CH_2)_n-$ scissoring mode at 1467 cm^{-1} is a medium intensity band. As shown in Fig. 6, the spectrum showed the presence of bands due to the C–O stretching vibration of esters between 1300 and 1100 cm^{-1}. These bands are slightly broader and weaker than the corresponding carbonyl absorption bands. The bands resulting from the methylene rocking vibration ρCH_2 appeared near 723 cm^{-1}.

In the FT-IR spectrum of AR57 (Fig. 6), characteristic broad band responsible for hydroxyl, amino stretching were observed around 3385 cm^{-1}. Aromatic and alkyl C–H stretching vibration were found at 3050 cm^{-1} and around 2950 cm^{-1}, respectively. The peaks at 1625 and 1491 cm^{-1} were assigned to aromatic C=C stretching vibration, while the peak at 1425 cm^{-1} corresponded to –N=N– bond stretching vibration. One other characteristic peak of this compound appearing at 1382 cm^{-1}, was attributed to ν(C–N) mode. According to the literature [40], the absorption bands of asymmetric and symmetric stretching of the O=S=O in $-SO_3H$ groups lie around 1350 and 1170 cm^{-1}, respectively. The absorption band of the stretching vibration of the S–O(H) in $-SO_3H$ groups lie around 907 cm^{-1}. Therefore, the changes of the bands found at 1340, 1173 and 900 cm^{-1} may be due to contributions from SO_3H groups. Furthermore, it seems that the shoulder and the peak exhibited at 1145 and 1195 cm^{-1} correspond to the absorption of symmetric and asymmetric stretching vibration of $-SO_3^-$.

FT-IR spectrum of synthesized microparticles show characteristic absorption bands of carnauba at 2920–2850 cm^{-1} for the aliphatic C–H stretching, bending and out of plane bending vibrations of CH_2 can be observed at 1463 and 720 cm^{-1}, the C=O vibration is also present at 1734 cm^{-1}. The broad overlapped peak at 3600–3200 cm^{-1} and the thin bands at 1336, 1170 and 918 cm^{-1} attributed to hydroxyl or amino and $-SO_3H$ stretching vibrations suggest the presence of the acid dye in the particles.

3.4. Morphology and particle size distribution of the double shell microparticles

Scanning micrographs of the microspheres loaded with acid dye revealed various shapes and particle sizes in the range of 1–5 µm (Fig. 7). It seems that the shape and the morphology of the microparticles are deeply influenced by the choice of the external polymeric shell. Thus, with a PE shell, the microparticles are well defined and have a spherical, smooth surface. During the coating with PS, the particles tend to aggregate before hardening. The resultant microparticles have rough surface with a raspberry-like morphology.

The difference between these two morphologies can be attributed to the miscibility of carnauba wax with PE according to the solubility parameters (15.8–17.1 $J^{1/2}/cm^{3/2}$ and 16.8 $J^{1/2}/cm^{3/2}$ for PE and carnauba wax respectively) in petroleum ether at high temperature. Whereas, the physico-chemical parameters of the PS coacervation phase (17.4–19 $J^{1/2}/cm^{3/2}$) do not allow the formation of an ideal binary mixture of these two compounds. It could be assumed from their surface morphology that PS and PE microspheres are suitable to the protection of the acid dye.

3.5. Thermal properties of microparticles

The thermal properties of various microspheres synthesized in this study and carnauba wax are shown in Table 2. The thermal properties

Table 2
Thermal properties of the various microspheres from DSC analysis (1 °C/min, N_2).

Sample	Melting			Crystallization			Dye content (%)
	T_{onset} (°C)	T_{peak} (°C)	ΔH_f (J/g)	T_{onset} (°C)	T_{peak} (°C)	ΔH_c (J/g)	
Carnauba wax	70.9	82.5	204.2	79.8	79.3	199.2	–
Acid dye/Carnauba wax microspheres	68.5	81.3	130.5	77.9	76.3	132.0	33.7–36.1
Carnauba wax/PE microspheres	69.6	86.3	183.4	77.9	73.4	174.7	–
Acid dye/Carnauba wax/PE microspheres	81.0	85.4	155.0	77.9	74.0	147.0	15.5–15.8
Carnauba wax/PS microspheres	72.1	83.6	161.4	78.3	75.7	149.0	–
Acid dye/Carnauba wax/PS microspheres	69.9	81.5	99.2	77.9	77.3	99.9	32.9–38.5

of the microspheres seem to be influenced by the outer polymeric shell. Thus, the temperature and the enthalpy of carnauba wax melting in the PE microspheres are higher than the other microspheres. During the formation of the shell, PE and carnauba wax are mixed together to create an interpenetrated network with a higher temperature of melting. Thus, the calculation of the PE content from the ratio of the enthalpies of carnauba/PE microspheres to carnauba wax reveals that the PE content (10.2–12.3%-wt) is close to the theoretical content (10.7%-wt) one. The measured enthalpy of PS microspheres is lower than the others. Furthermore, the difference between the theoretical (10.7%-wt) and the measured (21–25.2%-wt) content of PS can be due to a partial solubilization of the carnauba wax microspheres in toluene and therefore incomplete entrapment during the coacervation phase. Thus, microencapsulation using PE provides superior encapsulation of carnauba wax microspheres rather than using PS.

Three batches of microspheres containing acid dye with different compositions were synthesized and the loading contents are summarized in Table 2. The content of acid dye solution in the carnauba wax microspheres (first stage of preparation) according to DSC measurement is in the range of 33.7–36.1%; and after the second stage (formation of the outer shell), it decreases to 15.5–15.8% with a PE shell and it is about 32.9–38.5% with a PS coating. This value of the first stage is due to the loss of water and the partially removed acid dye after washing the microspheres. The same considerations can be applied to the PE microspheres, since the measured enthalpy is higher than the carnauba wax microspheres suggesting a loss of encapsulated acid dye solution (or water) at 80 °C. In the case of encapsulation with PS, the high value of dye content of microparticles obtained can be attributed to a loss of carnauba wax during the second stage.

3.6. Influence of the outer shell on microparticle coloration

From the calculation of the total colour difference (ΔE^*) of the dry microparticles (42.85 ($\pm$0.21) for carnauba wax microparticles, 56.24 ($\pm$0.35) and 40.30 ($\pm$0.29) for PE and PS double shell microparticles respectively), it seems that the encapsulation of acid dye reduces the colour perception. The difference of PS and carnauba microparticles can be attributed to the diffusion of the dye in the polymeric shell during the process. However the colour perception after heat revelation gives almost the same result for the PS microparticles and the PE microparticles, meaning close to the solid pigment ones. So this last heat transfer shows that the acid dye content (under solid form) in both microparticles is the same.

4. Conclusion

The aim of this study was to develop uncoloured microparticles containing a red acid dye in order to have, after heat transfer, the revealed red colour of the acid dye. Two polymers were used as outer coating materials, PE and PS. The process is divided in two consecutive steps. Firstly the emulsification of the dye solution in carnauba wax solutions and secondly, the entrapment of these particles according to a combined hot melt dispersion–coacervation method. Results from this study clearly show that the use of a gelatin solution as a protective colloid in combination with cyclohexan as solvent provided good results and allows to reduce the dye diffusion during the first stage of the microencapsulation process. The obtained microparticles are in the size range of 1–5 μm. The morphology of these particles was strongly affected by the chemical nature polymer used to coat the particles in the second step. Thus, the use of PE leads to a spherical, smooth surface while a rough surface with a raspberry-like morphology was found for PS. The shell colour was farther away from the solid pigment in the case of PE rather than in the PS case. In fact, the smooth surface morphology allows to contain the dye in the core of the microparticles, whereas during the formation of the PS microparticles, carnauba wax is partially swollen by the solvent inducing its partial solubilization and the dye diffusion through the shell. The acid dye content varies according to the process chosen. For the PE shell, the result decreased from 37 to 15% while for the PS shell, it was close to the carnauba microspheres ones, in the range of 32.9 to 38.5%. However, the colour perception after heat revelation allows to obtain a slighter difference. Therefore, it was determined that the encapsulation with a PE outer shell provided superior encapsulation of dye-microspheres rather than using PS.

References

[1] G. Nelson, Microencapsulates in textile coloration and finishing, Rev. Prog. Color. Relat. Top. 21 (1991) 72–85.
[2] K. Hong, S. Park, Preparation of polyurethane microcapsules with different soft segments and their characteristics, React. Funct. Polym. 42 (3) (1999) 193–200.
[3] C.P. Chang, T. Yamamoto, M. Kimura, T. Sato, K. Ichikawa, T. Dobashi, Release characteristics of an azo dye from poly(urea–urethane) microcapsules, J. Control. Release 86 (2003) 207–211.
[4] G. Nelson, Application of microencapsulation in textiles, Int. J. Pharm. 242 (2002) 55–62.
[5] K. Hong, S. Park, Preparation of polyurethane microcapsules with different soft segments and their characteristics, React. Funct. Polym. 42 (3) (1999) 193–200.
[6] C.C. Pong, M. Kimura, T. Yamamoto, M. Nobe, T. Dobashi, Effect of dispersing medium on permeability of microcapsule membrane, Colloids Surf., B Biointerfaces 30 (1–2) (2003) 123–127.
[7] S. Takashi, T. Yamamoto, S. Shibako, K. Ichikawa, T. Dobashi, Permeability of azo-dye through poly(urea–urethane) microcapsule membrane, J. Membr. Sci. 213 (1–2) (2003) 25–31.
[8] C.P. Chang, T. Yamamoto, M. Kimura, T. Sato, K. Ichikawa, T. Dobashi, Release characteristics of an azo dye from poly(urea–urethane) microcapsules, J. Control. Release 86 (2003) 207–211.
[9] H. Shinyoung, Y. Yang, Antimicrobial activity of wool fabric treated with curcumin, Dyes Pigm. 64 (2) (2005) 157–161.
[10] C.C. Pong, J.C. Chang, K. Ichikawa, T. Dobashi, Permeability of dye through poly (urea–urethane) microcapsule membrane prepared from mixtures of di- and tri-isocyanate, Colloids Surf., B Biointerfaces 44 (4) (2005) 187–190.
[11] M.M. El-Zawahry, S. El-Shami, M.H. El-Mallah, Optimizing a wool dyeing process with reactive dye by liposome microencapsulation, Dyes Pigm. 74 (3) (2007) 684–691.
[12] A. Maza, J.L. Parra, A. Manich, Lipid bilayers including cholesterol as vehicles for acid dyes in wool dyeing, Tex. Res. J. 63 (1993) 643–649.
[13] J.R. Gomes, L.F.A. Baptista, Microencapsulation of acid dyes in liposomic structures of lecithin and surfactants, Tex. Res. J. 71 (2001) 153–156.
[14] L.Y. Chu, S.H. Park, T. Yamaguchi, S.I. Nakao, Preparation of thermo-responsive core-shell microcapsules with a porous membrane and poly(N-isopropylacrylamide) gates, J. Membr. Sci. 192 (1–2) (2001) 27–39.
[15] N. Sarier, E. Onder, The manufacture of microencapsulated phase change materials suitable for the design of thermally enhanced fabrics, Thermochim. Acta 452 (2) (2007) 149–160.
[16] D. Aitken, S.M. Burkinshaw, J. Griffiths, A.D. Towns, Textile applications of thermochromic systems, Rev. Prog. Color. 26 (1996) 1–8.
[17] L.D. Small, G. Highberger, Thermochromic ink formulations, nail lacquer and methods of use. Chromatic Technologies United States Patent 5 997 849, 1999.
[18] T. Kidchob, S. Kimura, Y. Imanishi, pH-responsive release from polypeptide microcapsules, J. Appl. Polym. Sci. 63 (4) (1997) 453–458.
[19] K. Sawada, H. Urakawa, Preparation of photosensitive color-producing microcapsules utilizing in situ polymerization method, Dyes Pigm. 65 (1) (2005) 45–49.
[20] S.J. Chang, C.H. Lee, C.Y. Hsu, Y.J. Wang, Biocompatible microcapsules with enhanced mechanical strength, J. Biomed. Mater. Res. 59 (1) (2002) 118–126.
[21] H. Guo, X. Zhao, J. Wang, Synthesis of functional microcapsules containing suspensions responsive to electric fields, J. Colloid Interface Sci. 284 (2) (2005) 646–651.
[22] A. Voigt, N. Buske, G.B. Sukhorukov, A.A. Antipov, S. Leporatti, H. Lichtenfeld, H. Baumler, E. Donath, H. Mohwald, Novel polyelectrolyte multilayer micro- and nanocapsules as magnetic carriers, J. Magn. Magn. Mater. 225 (1–2) (2001) 59–66.
[23] F. Salaün, E. Devaux, S. Bourbigot, P. Rumeau, Preparation of multinuclear microparticles using a polymerization in emulsion process, J. Appl. Polym. Sci. 107 (4) (2008) 2444–2452.
[24] F. Salaun, I. Vroman, Influence of core materials on thermal properties of melamine-formaldehyde microcapsules, Eur. Polym. J. (in press).
[25] J. Pollauf, W. Pack, Use of thermodynamic parameters for design of double-walled microsphere fabrication methods, Biomaterials 27 (14) (2006) 2898–2906.
[26] D. R. Gomes, J. Isidoro United States Patent Application 20060188582 A1, 2006.
[27] N.A. Rahman, E. Mathiowitz, Localization of bovine serum albumin in double-walled microspheres, J. Control. Release 94 (1) (2004) 163–175.
[28] R. Langer, E. Mathiowitz, Preparation of multiwall polymeric microcapsules, United States Patent 4 861 627, 1989.
[29] B. Gander, P. Johansen, H. Nam-Tran, H.P. Merkle, Thermodynamic approach to protein microencapsulation into poly(D,L-lactide) by spray drying, Int. J. Pharm. 129 (1–2) (1996) 51–61.
[30] A. Asperger, W. Engewald, G. Fabian, Advances in the analysis of natural waxes provided by thermally assisted gydrolysis and methylation in combination with GC/MS, J. Anal. Appl. Pyrol. 52 (1999) 51–63.

[31] M. Regert, J. Langlois, S. Colinart, Characterisation of wax works of art by gas chromatographic procedures, J. Chromatogr. 1091 (1–2) (2005) 124–136.
[32] R.F. Fedors, A method for estimating both the solubility parameters and molar volumes of liquids, Polym. Eng. Sci. 14 (1974) 147–154.
[33] L. Wang, S. Ando, Y. Ishida, H. Ohtani, S. Tsuge, T. Nakayama, Quantitative and discriminative analysis of carnauba waxes by reactive pyrolysis-GC in the presence of organic alkali using a vertical microfurnace pyrolyzer, J. Anal. Appl. Pyrolysis 58–59 (2001) 525–537.
[34] J.P. Teas, Graphic analysis of resin solubilities, J. Paint Technol. 40 (516) (1968) 19–25.
[35] G.E. Means, R.E. Feeney, Chemical Modification of Proteins, Ed. Holden-Day Inc., Chap. 3, 35–51, 1971.
[36] C.A. Finch, in: C.A. Finch (Ed.), Chemistry and Technology of Water-soluble Polymers, Plenum Press, New York, 1983, pp. 81–112, Chap. 5.
[37] C.B. Hudson, Gelatine – relating structure and chemistry to functionality, in: K. Nishihari, E. Doi (Eds.), Food Hydrocolloids: Structures, Properties, and Functions, Plenum, New York, 1994.
[38] J. Poppe, Gelatin, in: A. Imeson (Ed.), Thickening and Gelling Agents for Food, 2nd ed., Blackie Academic and Professional, London, 1997, pp. 144–168.
[39] E.N. Dubis, A.T. Dubis, J.W. Morzycki, Comparative analysis of plant cuticular waxes using HATR FT-IR reflection technique, J. Mol. Struct. 511–512 (1999) 173–179.
[40] W. Chen, J.A. Sauer, M. Hara, The effect of ionic cross-links on the deformation behavior of homoblends made of poly(styrene-co-styrenesulfonic acid) and poly (styrene-co-4-vinylpyridine), Polymer 44 (25) (2003) 7729–7738.